Notch signalling plays a critical role in patterning the ventral mesoderm during early embryogenesis in *Drosophila melanogaster*

Abstract:

Notch signaling is a critical regulator of multiple developmental processes through its ability to control gene expression, and thereby influence cell fate specification and cell proliferation through direct cell-cell communication. Although Notch signalling has been implicated in myogenesis during late embryogenesis, the role of Notch signalling in early mesoderm development in largely unexplored. Endocytosis of the ligand and receptor extracellular domain is observed in the mesoderm and mesectoderm and therefore indicative of signalling activity. Here we present evidence that critical mesodermal genes require and are responsive to Notch signalling activity. We also developed a novel light-inducible variant of NICD to allow precise control of ectopic activation of Notch signalling. Using a combination of high-resolution fluorescent mRNA *in situ* hybridizations and qPCR, we identified a set of mesodermal genes that are directly regulated by Notch signalling. We also show evidence that Notch signalling indirectly regulates the dorsal- ventral patterning program mediated by the Toll signalling pathway through the Dorsal/ Twist/ Snail network. Our findings in this paper show that Notch signalling regulates mesoderm patterning and boundary formation between it and the ectoderm by regulating the expression of critical genes and providing negative feedback on the upstream patterning network.

Introduction:

Embryogenesis is a critical developmental process that is driven by patterns of gene expression, which collectively organize the coordinated cell proliferation and differentiation required for proper organismal development[1]. *Drosophila melanogaster* has been used as a model organism to study the critical mechanisms that direct embryogenesis[1]. It has also served as a very useful model system to study signalling pathways that coordinate body patterning and morphogenetic movements that form primordial organs which then give rise to different structures of the organisms[2].

Embryonic development can be divided into four main stages; cleavage, blastulation, gastrulation, and neurulation[3]. The first stage, cleavage, involves many cell divisions that form the blastula from the single-cell zygote[3]. Blastulation results in the formation of the blastula through many cell divisions[3]. Some differentiation takes place at the end of blastulation but it is not significant[3]. Gastrulation is the development of the three germ layers; the ectoderm, the mesoderm, and the endoderm[2]. The ectoderm forms the outermost layers of the organism; surface ectoderm, neural crest, and the neural tube[4].The mesoderm forms the mid-layer of the organism, which later develops into muscle, bone, cartilage, circulatory and lymphatic system, connective and adipose tissue, the notochord, dermis, serous membranes, and the genitourinary system[4]. Finally, the last stage, neurulation is the development of the neural tube of vertebrates[4]. During early embryogenesis of *Drosophila melanogaster* 13 nuclear division cycles occur within the same cytoplasm[3]. This early development is instructed by maternally deposited mRNAs and proteins that organize the anterior-posterior and dorsal-ventral body axes and define the

segmental pattern of the embryo that later gives rise to different body segments of the larval and adult stages[5]. This early body plan is then refined by functional products from the zygote's genome[5]. During the 14th nuclear cycle, individual cell membranes form to separate individual nuclei, this stage is referred to as cellularization[3]. The maternally deposited materials are degraded during this stage and the control of development is handed off to the zygote through the activation of zygotic transcription[6,7]. The cells located in the ventral most region of the cellularized blastoderm make up the presumptive mesoderm, which undergo a series of cell shape changes; apical flattening, apical constriction, shortening along the apico-basal axis, followed by cell depolarization, dispersion and migration along the ectoderm, where they attach[2,4]. Cell shortening along the apico-basal axis results in ventral furrow invagination and eventually the mesoderm forms a tube along the anterior-posterior axis of the embryo that is then internalized[2]. Once it is fully internalized, FGF signalling between these cells and the underlying ectoderm cells facilitates mesoderm collapse against the ectoderm cells[8]. These cells then lose polarity and transition to become mesenchymal cells and divide twice[8]. Then FGF signalling facilitates cell migration and spreading along the ectoderm to form a single layer of cells, called a monolayer[8].

Notch signalling is critical to cell proliferation, differentiation, and to the development of virtually all the different tissues that give rise to the adult organism[1]. It is also essential to the development of both vertebrates and invertebrates[9]. For example, it has been previously shown that *Drosophila melanogaster* embryos homozygous for loss-of-function Notch alleles do not reach adulthood[10]. The Notch receptor, a transmembrane protein, is activated by the binding of its ligand (Delta) on neighbouring signal-sending cells, followed by ligand internalization and Notch receptor activation through transmembrane cleavage[1]. Notch cleavage allows for Notch intracellular domain (NICD) release from the plasma membrane, allowing transport to the nucleus where it regulates gene expression through removal of a gene repressor, suppressor of hairless (Su(H)), from Notch target genes[1]. Ligand internalization has been previously shown to be necessary for Notch activation[1]. Endocytosis of Delta and the extracellular domain of the Notch receptor is observed in all mesodermal cells (Fig 1), indicating Notch signalling is active in the adjacent cells[11]. Although the role of Notch signalling during embryogenesis is well studied, little is known about its role in the development of the mesoderm[1]. Likewise, the identity of Notch target genes in the ventral mesoderm is not yet known. Here we show that Notch signalling is active in the presumptive mesoderm and is required for proper progression through gastrulation. We identified a set of Notch target genes that are expressed in the mesoderm and characterize their expression in gain-of-function and loss-of-function mutant embryos of the Notch pathway. In this work we developed and characterized a novel tool to ectopically activate Notch signalling in a temporally precise light-inducible manner. Our findings also support a mechanism whereby Notch signalling provides negative feedback unto the early patterning Toll pathway, and thereby affecting the Dorsal/ Twist/ Snail network. Together, our work demonstrates that Notch signalling plays a critical role in the formation of the mesoderm and the boundary separating it from the ectoderm during early embryogenesis.

Results:

Delta endocytosis and NECD transendocytosis in the mesoderm and identification of candidate Notch target genes in the mesoderm

The role of Notch signalling in during embryogenesis has been well characterized in the lateral ectoderm and the mesectoderm. In the lateral ectoderm, Notch signalling works in concert with EGF and Toll signalling to coordinate neurogenesis. In the mesectoderm, Notch signaling is required to form the boundary between the ectoderm and mesoderm by activating target genes such as *sim*. Although there's evidence of Notch activity in the mesoderm (Fig 1B), its potential role has not yet been elucidated. It has been shown that Delta endocytosis is necessary for Notch signalling to occur[11,12,13]. This is internalization of Delta and trans-endocytosis of NECD is observed in the presumptive mesoderm cells (Fig 1B), which indicates that Notch signalling is active in these cells[11]. Traditionally, expression of *sim* and *m8* have been used as a readout of Notch signaling in the early embryo[14]. However, since both genes are actively repressed in the mesoderm by Snail, a transcriptional repressor that coordinates mesoderm formation, the activity of Notch signalling in the presumptive mesoderm may have been overlooked[14]. When Snail repression is removed as in *snail*$^{-}$ mutants, *sim* RNA is detected in the mesoderm[15]. We aimed to investigate the role of Notch signalling in the presumptive mesoderm. To address this, we first created a list of candidate transcriptional targets of Notch signalling and analyzed their expression in loss of function Delta mutants. To do this we used the BDGP *in situ* data, modENCODE RNA-seq data, and analyzed previously published suppressor of hairless CHIP-seq data to select genes that are expressed in the presumptive mesoderm of cellular blastoderms, exhibit differential expression during nc. 14 (which coincides with the increase of Notch signalling activity) and which contain a suppressor of hairless binding site in their promoter region[16,17,18]. We determined that the following genes are candidate transcriptional targets of the Notch signalling pathway; *Asph*, *Twist*, *Tinman*, *Traf4*, *WntD*, *Stumps*, *String*, *Heartless*, *NetrinA*, *Neurotactin*, *mir-1*, *Mes2*, and *Mef2* (Figure 1C).

Notch signalling is required for the expression of critical mesodermal genes

We employed homozygous null Delta mutant alleles to test the necessity of Notch signalling to the development of the ventral mesoderm. We used two orthogonal methods, Fluorescent RNA *in situ* hybridization (FISH) and quantitative real-time PCR (qPCR), against twelve candidate mesodermal Notch target genes that we have identified through *in silico* analysis.

We found that there are three classes of genes within this set of candidates based on their expression level in the absence of Notch signalling (Figure 2):

1) Whose expression requires Notch signalling. These include: *Asph*, *Mef2*, *Mes2*, *Neurotactin*, *String*, *Stumps*, *Tinman*, *Traf4*, *Twist* (Fig 2A, 2D),
2) Whose expression is repressed by Notch signalling; *Heartless* and *WntD* (Fig 2B, 2E)
3) Whose expression is independent of Notch signalling, *NetrinA* (Fig 2C, 2F)

For all but one gene we did not observe significant changes in the position of expression between wildtype and Delta mutant embryos. However, *WntD* was expressed at higher levels in the mesoderm of Delta mutants compared to wildtype but expression in the mesectodermal cells was significantly reduced compared to its wildtype counterparts (Fig 2B).

Development of Opto-NICD allows titration of ectopic Notch signalling activity and incremental expansion of *Sim* expression

These findings motivated us to test whether Notch signalling is sufficient to drive expression of these genes. We sought to develop a tool that allows us to ectopically activate Notch signalling with precise temporal control. We engineered a light-inducible variant of the NICD (Opto-NICD) and expressed it in the early embryo. In this system, prior to photoactivation with blue light (488 nm), OptoNICD is tethered to the membrane. Upon photoactivation, NICD is cleaved by a light-inducible TEV protease, and translocates to the nucleus where it can relieve gene repression (Fig 3A). We first tested this in S2 cells. Prior to photo activation OptoNICD (tagged with GFP) was localized to the membrane and internal membranous structures but excluded from the nucleus. One hour after photoactivation, Opto-NICD-GFP can be detected in the nucleus (Fig 3B). Next, we expressed our construct in the early embryo. We used *sim* expression as a readout for Notch signalling levels because it is a direct target of Notch signalling. Its expression domain has previously been shown to expand beyond the mesectoderm cells as a result of overexpression of NICD[14]. As predicted, prior to photoactivation, Notch signalling activity is at similar levels to wildtype embryos, as only endogenous Notch signalling is active (Fig 3C). We also show that we can control the extent of over activation by varying the time that these embryos are exposed to light (Fig 3C, 3D). Embryos exposed to 10 minutes of light exhibited the smallest expansion in *sim* expression (this was only seen in mid nc 14 embryos- shown in the *in situ* not embryos at cephalic furrow- represented in the qRT-PCR data) (Fig 3C, 3D). Incremental expansions were seen in *sim* expression that coincide with amount of time the embryos were exposed to light (with the exception that *sim* expression was higher in 1 hour than 2hours of light exposure) (Fig 3C, 3D). This could be due to negative feedback mechanisms, downregulating *sim* expression. After 1 hour of light exposure, the embryos expressed *sim* in the presumptive mesoderm and the number of cells that did not contain *sim* mRNA was decreased significantly compared to wildtype embryos (~ 8 cells at the most, 0 in some areas along the AP axis). This was also seen in embryos exposed to light for 2 hrs but to a lesser extent (~ 10 cells at the most, 0 around the cephalic furrow) (Fig 3C, 3D). This suggests that moderate levels of Notch signalling activity are required for mesodermal gene expression.

We also observed morphological defects in embryos exposed to light for 1 (not shown) and 2 hours (Fig 3E). The embryos had ectopic invaginations along the AP axis during early stages of gastrulation, where the ventral furrow is forming but the mesoderm is not fully internalized. After the internalization of the mesoderm, the cephalic furrow appears closer to the middle of the mutant embryo along the AP axis compared to wildtype counterparts. There are also additional invaginations along the AP axis on the ventral side. At older stages that roughly

correspond to germband retraction, the mutant embryo is twisted much like loss-of-function Twist mutant embryos (Fig S1).

Ectopic Notch signalling is detrimental to mesoderm formation and decreases mesodermal gene expression

To test whether Notch signalling activation is sufficient to drive the expression of the mesodermal genes, we activated Notch signalling using our Optogenetic system in the early embryo and examined mesodermal gene expression using FISH and qRT-PCR. We photoactivated nc 9-10 embryos expressing both components of the system by exposing them to light, using an LED light box, for 2 hours and 20 mins continuously.

We found that there are two classes of genes within this set of candidates based on their expression level in the absence of Notch signalling (Fig 4):

1) Whose expression is repressed by Notch signalling overactivation. These include: *Asph*, *Mef2*, *Mes2*, *Neurotactin*, *String*, *Stumps*, *Tinman*, *Traf4*, *Twist*, and *NetrinA* (Fig 4A-B).
2) Whose expression is significantly upregulated and expression domain is expanded outside of the mesoderm and mesectoderm (in the case of *WntD*): *String* and *WntD* (Fig 4C-F)

In wildtype embryos, *WntD* is not expressed in the ectoderm but expressed in all the mesectoderm cells at higher levels than the mesoderm and is not expressed in all mesoderm cells across the anterior-posterior axis. Rather *WntD* is expressed in mesoderm cells at low levels in a segmented pattern (Fig 4E). This expression pattern is a distinguishing feature of the mesoderm cells. However, in Opto-Notch embryos, expression in the mesectoderm cells becomes more similar to neighbouring mesoderm cells as Notch signalling is increased and expression is detected in ectoderm cells. *WntD* expression was increased in Opto-Notch embryos that were photoactivated for 30 mins in the mesoderm but was still segmented and this pattern was distinct from that of neighbouring mesectoderm cells, where *WntD* was expressed in a continuous 2-3 cell wide stripe across the AP axis. In contrast, *WntD* was expressed in mesoderm, mesectoderm, and ectoderm cells in a segmented pattern across the AP axis of Opto-Notch embryos photoactivated for 1 hour, which had the highest levels of Notch signalling, as seen by the *sim* expression (Fig 3). Ectopic Notch signalling alters the expression profile of mesoderm, mesectoderm and ectoderm cells and therefore these cells are less distinguishable from one another. This emphasizes the role of Notch signalling in boundary refinement.

Our observation that mesoderm and mesectoderm/ectoderm expression of *WntD* expression is differentially regulated by Notch signalling drove us to further investigate the regulatory relationship between Notch signalling and *WntD*. We hypothesized that the increase in mesoderm *WntD* expression in D^- mutants observed (Fig 2B, 2E) may be due to indirect regulation in the mesoderm and the increases in expression outside the mesoderm in N^+ embryos is likely due to Notch-dependent removal of gene repression. Since *WntD* is a target of the

Dorsal/Twist/Snail network and has been shown to negatively regulate Dorsal activity by decreasing its nuclear translocation, we decided to investigate whether decreases or increases in Notch signalling affect the mRNA and protein expression of Twist and Snail as well as Dorsal protein expression and distribution across the D-V axis.

Notch signalling regulates *Twist* and *Snail* expression

Twist and Snail are two critical master regulators of gastrulation[2,4,19]. Twist is a transcription factor that is necessary for the expression of most mesodermal genes involved in gastrulation, while Snail is a gene repressor that inhibits the expression of genes that specify other tissues such as the mesectoderm and the ectoderm[4,19]. We analyzed embryos at cellularization to determine the number of cells in the mesoderm, cells expressing Twist. We found that the number of Twist positive cells of loss-of-function Delta mutants (D^-) and gain-of-function (N+) Notch mutants are significantly reduced (Fig 5A, 5C). During later stages of gastrulation, both D^- and N^+ mutants show developmental defects, which resemble the Twist loss-of-function mutant phenotype (Fig S1). The reduced protein expression is supported by reduced gene expression of these mutants compared to their wildtype counterparts (Fig 5B). We also analyzed Snail expression at the mRNA and protein level. In D^- mutants, *snail* mRNA expression is significantly increased while in N^+ mutants, *snail* mRNA expression is significantly increased (Fig 5F, 5G). This indicates that Notch signalling negatively regulates *snail* expression. The number of Snail positive cells during cellularization was significantly reduced in D^- and N^+ mutants (Fig 5D, 5E). The number of Snail-positive cells are similar to the Twist-positive cells. The discrepancy between Snail protein and mRNA expression in D^- mutants indicates that there are two distinct inputs from Notch signalling. This indicates that increases and decreases in Notch signalling during early cellularization results in a decreased mesoderm domain. Put together, this data supports the hypothesis that Notch signalling is active in the mesoderm and is required for mesodermal gene expression and proper progression through gastrulation.

These results also indicate that there may be an input from Notch signalling on Dorsal distribution and thereby its activity. We then analyzed the expression of Dorsal during cellularization in wildtype embryos, loss-of-function, and gain-of-function counterparts.

Notch signalling provides a negative feedback signal on Dorsal distribution by regulating *WntD* expression

Dorsal is a transcription factor, part of the Toll signalling pathway, that is maternally deposited and forms a morphogen gradient across the Dorsal-Ventral axis[20]. It is critical for establishing polarity along the Dorsal-Ventral axis[20]. In the absence of Toll signalling, Dorsal is bound to a protein named Cactus in the cytoplasm and inhibited from entering the nucleus[21]. Once Toll signalling is activated by Spätzle (Spz), Cactus is targeted for destruction, liberating Dorsal which then translocates to the nucleus, where it activates gene expression[22,23]. The nuclear amount of Dorsal is most concentrated in the ventral most region of the blastoderm, which results in activation of genes requiring strong activation by Dorsal such as the two master regulators of gastrulation; Twist and Snail[2,4,19,24]. We found that the number of cells with a

highest concentration of Dl is significantly reduced in D^- and N^+ mutants (Fig 6A, 6B). Interestingly, we found that some N^+ mutants showed a stronger Dl signal, that corresponded to a higher number of cells with a high Dl concentration, while others that showed a much lower Dl signal that corresponded to a lower number of cells with high Dl concentration (Fig 6A, 6B). This suggests that Notch signalling negatively regulates Dl distribution in the mesoderm as when Notch signalling is increased mesodermal cells no longer contain the highest concentration of Dl protein. This result explains the reduced expression of both Twist and Snail protein levels in Notch mutants (Fig 5). A decrease in ventral Dl concentration, results in reduced expression of target genes, *Snail* and *Twist*. Since Dorsal activity normally precedes Notch signalling during early embryogenesis, we propose that Notch is acting on the Dorsal/Twist/Snail network through an intermediate negative regulator. Here we show strong evidence that Notch signalling upregulates *WntD* expression. As WntD inhibits Dorsal nuclear localization, the increase of *WntD* expression leads to decreases in Dl nuclear localization and transcriptional activation of target genes including *Twist* and *Snail*[25].

Discussion:

Disentangling the role of Notch signalling during early embryogenesis is critical to understanding the mechanisms involved in tissue formation and boundary establishment and refinement. The processes involved in tissue and boundary formation are conserved in later stages of the organism's life as in stem cell renewal and differentiation. Unraveling the interactions between different signalling pathways such as Notch signalling and Toll signalling is also important for understanding disease pathogenesis, where the same processes are misregulated and lead to disease[26].

The role of Notch signalling during embryogenesis has long been appreciated in the context of neurogenesis and myogenesis, which both occur after early mesoderm development[27,28]. However, while there's evidence to suggest that it is active in the mesoderm, its role here is largely unexplored. There have been very few genetic links characterized between Notch and genes expressed in the mesoderm, although these links are observed in adult tissues or during neurogenesis and myogenesis during later stages of embryogenesis and larval stages[29,30]. Notch has been shown regulate the expression of; *Twi*, *Asph*, and *string*[29,30]. Here, for the first time, we present evidence of its activity in the ventral presumptive mesoderm and identify target genes, which are critical to mesoderm formation and gastrulation, that are dependent on Notch signalling for their expression. Among these genes are; *tinman*, *Mes2* and *Mef2* which all encode transcription factors that are necessary for myogenesis during embryonic and larval stages[31,32,33,34,35,36]. Some of the genes, whose expression was dependent at least in part on Notch signalling were factors that are involved in orchestrating or facilitating cell shape changes that are necessary for mesoderm invagination and internalization[37]. These include; *Traf4*, which encodes a cytoplasmic protein involved in TNF signalling, which plays a critical role in the cellular apical constriction, which is necessary for ventral furrow invagination[37]. Another affected gene, Neurotactin, encodes a cell adhesion molecule[38]. Decreases and increases in Notch signalling also affect the expression of *htl* and *stumps*, which encode key players of FGF signalling, which is required for mesoderm spreading[8]. Here we show that Notch signalling is

required for the expression of *Stumps* but negatively regulates *htl* expression. Although the loss-of-function mutants did not show defects in mesoderm spreading when cross-sections were examined. This indicates that expression of these genes is only partially dependent on Notch signalling, which is consistent with previous studies that characterized them as target of Twist[34.39,40]. Since Twi protein is expressed in these loss-of-function Delta mutants, this indicates that the Twi protein reductions observed are not detrimental and are sufficient for some downstream target gene expression and therefore do not perturb mesoderm spreading.

To test the sufficiency of Notch signalling to drive the expression of mesodermal genes, we developed a novel light-gated tool that allows precise temporal control. This system provides several advantages compared to traditional overexpression models that have been used previously; 1) The system is titratable as shown by the incremental expansion of *sim* expression (Fig 3), 2) the combination of this system with tissue-specific gal4 drivers can provide tissue specific and temporal control, and 3) it has the potential to allow precise spatial control if combined with light sheet microscopy. For our experiments, it allowed us to have temporal control of activation of the system according and to titrate Notch activity. There are a few cells in the embryo that did not express *sim* in regardless of photoactivation time, which indicates that there are additional regulatory mechanisms that either directly repress *sim* or indirectly by inhibiting NICD translocation to the nucleus.

In this study, we present evidence that critical mesodermal genes require Notch signalling for normal expression, shown by significant decreases in mesodermal gene expression in both loss-of-function and gain-of-function Notch mutant embryos. In the gain-of-function Opto-Notch mutants that were photoactivated for a longer duration, expression of most of the mesodermal target genes was significantly reduced (Fig 4), however expression in those photoactivated for shorter durations was significantly increased for many of the candidate genes including; *Mes2*, *Tinman*, *Stumps*, *Twist*, *Mef2*, and *NetA* (Fig S2). This indicates that Notch is sufficient to increase their expression, and that different genes require different levels of Notch signalling. The decrease in expression after a long duration of photoactivation is likely due to two reasons; 1) negative feedback inhibition inputs that follow increases in gene expression, some of which from Notch target genes encoding gene repressors, (E(spl)C and potentially emc)[29] and 2) decreases in *Twist* expression, as most of these genes are also transcriptional targets of Twist[34]. Our findings are supported by previous experiments preformed later in gastrulation that showed that Notch signalling regulates Twist expression directly through activating expression and indirectly by activating the expression of repressors of Twist[29].

Some of the mesodermal genes were downregulated following Notch overactivation regardless of photoactivation duration including; *Asph*, *Neurotactin*, *Traf4*, and *Heartless*. Although these genes contain consensus Su(H) binding sites in their extended gene regions, our expression analysis indicates that Notch signalling is not sufficient to increase their expression in the mesoderm. This is likely due to their repression by other Notch target genes such as the E(spl)C genes, such as Emc, although this has not been tested here. Another likely mechanism is negative feedback through post-translational modifications of the endogenous NICD and Opto-NICD proteins that lead to their degradation[41,42]. This is supported by the decrease in fold-

change of *sim* expression in the embryos that are photoactivated for 2 hours compared to 1 hour (Fig 3). Put together, these findings provide clear evidence that Notch is normally active in the mesoderm during early embryogenesis and is required for normal levels of mesodermal gene expression. This requirement of Notch signalling is emphasized by the defects observed in later stages of gastrulation (after the internalization of the mesoderm) of loss-of-function mutants (Fig 5).

Interestingly, we identified one gene, *string*, that behaves as a classic direct target of Notch signalling; its expression is significantly reduced in the absence of Notch signalling and is significantly increased upon overactivation of Notch signalling. *String* encodes a phosphatase, cdc25/ String, that activates a mitotic kinase, cdk1[43,44]. Zygotic cell division is dependent on *stg* expression[42,43]. Loss-of-function mutants exhibit cell cycle arrest after nuclear cycle 14, which is the last cycle controlled by maternally deposited String, however, cell shape changes and morphogenetic movements are not affected except that cell numbers in the mesoderm are reduced[43,44]. The precise temporal expression of *string* has been shown to critical for the coordination of cell division[43,44]. The morphological defects observed in the N^+ mutants described here may also be due to premature accumulation of *string*, causing premature cell division prior to mesoderm internalization.

Interestingly, we identified a gene, *WntD*, that is differentially regulated by Notch signalling across neighbouring tissues; the mesoderm and mesectoderm. Our expression analysis of loss-of-function mutants indicates that Notch signalling is required for *WntD* expression in mesectoderm cells that flank mesoderm cells on both sides, while it negatively regulates its expression in the mesoderm, as seen by the increase in expression in this region in the absence of Notch signalling activity (Fig 2). The presence of Su(H) consensus binding sites in the *WntD* genomic region indicates that Notch can activate its expression directly by binding to Su(H). This is likely the main input on *WntD* in the mesectoderm. Our results imply that Notch activates the expression of a repressor of *WntD* in the mesoderm and in the absence of Notch signalling, this repression is relieved. The identity of this repressor remains unclear. In the gain-of-function mutant expression of *WntD* is expanded laterally beyond the mesectoderm, much like that of *sim* in those embryos and the boundary between the mesoderm and ectoderm becomes much less defined. This finding highlights the role of Notch signalling in defining the boundary between different tissues. Increases or decreases in Notch signalling, results in changes in the expression profile of these boundary cells. In the loss-of-function mutants, they lose expression of *WntD* and *sim*, while in GOF mutants, the are no longer distinct from neighbouring cells, as they express these two genes at similar levels to the neighbouring mesoderm and ectoderm cell. These changes of expression profile most likely contribute to the defects in the embryonic midline observed in the GOF mutants.

WntD encodes a secreted ligand of the Wnt family of proteins and has been identified as an inhibitor of Dorsal[25]. It has been shown that its expression is regulated by the Dorsal-Twist-Snail genetic network, and provides negative feedback by competitively binding to the Toll receptor instead of Spz and preventing Dl nuclear transport[45]. Our finding that increases in *WntD* expression coincide with decreases in the size of the region with the most concentrated Dorsal

protein supports previous findings[45]. As expected, the decrease of this region, where Dorsal is most highly concentrated results in decreases in Snail- and Twist- positive cell numbers. This indicates that the mesoderm region is narrowed in both loss- and gain-of-function mutants, which emphasizes the role of Notch signalling in the development of the mesoderm. Put together, these findings provide evidence that in addition to functioning in a cell-autonomous manner to drive mesodermal gene expression, Notch signalling also provides feedback inhibition signals on the upstream patterning programme, regulated by Toll signalling through Dorsal, indirectly by regulating *WntD* expression.

Conclusion:

In conclusion, here we show that Notch signalling plays a dual role during early mesoderm development in embryogenesis. Notch activity drives gene expression of critical mesoderm genes and simultaneously provides negative feedback regulation by activating expression of at least one inhibitor of mesodermal gene expression, *WntD*, to maintain appropriate levels of gene expression in the mesoderm. In addition, we describe the development of a novel light-gated tool that allows precise temporal ectopic activation of Notch signalling. Lastly, we present evidence of a negative feedback on Dorsal, the master regulator of gastrulation, regulated by Notch signalling and show the role of Notch signalling in boundary refinement.

Future directions and limitations:

While we show that WntD is differentially regulated by Notch signalling across different tissues, we have not identified the potential repressor that is activated in the mesoderm by Notch signalling. In addition, we would like to continue to characterize the morphological defects observed in our mutant embryos by analyzing the expression of cell adhesion molecules and cytoskeletal proteins that are critical to mesoderm internalization and spreading.

Methods:

Analysis of ChIP-seq data for Su(H) binding sites in mesodermal genes

First we generated a list of genes that were expressed in the mesoderm and were differentially expressed at nuclear cycle 14 of embryogenesis based on mRNA expression profiles available on BDGP and RNA-seq data from the modEncode project[16].

To determine Su(H) binding sites in the extended regions of the genes of interest, we analyzed ChIP-seq data generated by Ozdemir et al. (2014)[18]. The study generated Su(H) ChIP-seq data for 2–4-hour yw embryos using goat and rabbit antibodies. To predict Su(H) binding sites, we separately analyzed the data generated by the replicate experiments with the two antibodies and finally combined the findings to get the non-redundant list of Su(H) binding sites for every gene.

The wig files were retrieved from Gene Expression Omnibus (GEO) (GEO accession: GSE59726). The wig files were converted to bigwig format which were then converted to bedgraph format using the tools wigToBigWig and bigWigToBedGraph respectively. We further used the MACS3 peak caller (Feng et al., 2011) to call peaks using bedgraph files[46]. The 20bp region surrounding the point source of peak was taken as the binding site. The predicted Su(H) binding sites were intersected with the extended regions of genes using bedtools (Quinlan and Hall, 2010) to get Su(H) binding sites on the genes' extended regions[47].

Fly crosses and transgenic lines:

Flies were maintained at 25 ^{o}C and fed with semi-defined food made as described[48]. Most of the stocks used here were obtained from the Bloomington Stock Center or were gifted by other labs as outlined in Table S1.

W1118 flies were used as wildtype controls. Delta-TS contain are heterozygous for two temperature sensitive alleles of Delta, which is fully functional at 25 ^{o}C but non-functional at 32 ^{o}C[49]. Resultant embryos from Delta-TS flies were collected for 1.5 hours, then heat- shocked at 32 ^{o}C for 2 hours and 20 minutes and then fixed and stored in methanol at -20 ^{o}C.

We used the Best Gene injection services to generate our transgenic fly lines using Φ C31-mediated attp/attB transgenesis. The mCD8-CIBN-NTEV-NICD-GFP transgene was inserted using the attP40 insertion site on chromosome 2 and balanced over CyO, while the Cry2-CTEV-mCherry transgene was inserted using the attP2 insertion site on chromosome 3 and balanced over TM3.

To generate OptoNICD embryos, homozygous UASp> Cry2-CTEV-mCherry virgin female were crossed to homozygous UASp>mCD8-CIBN-NTEV-NICD-GFP males. Males and females from the resultant generation (heterozygous for both alleles) were crossed and their progeny was screened for double homozygote virgin females which were crossed to male Mat- alpha- tublin> Gal4 flies. The females from this progeny, whose genotype was {[y1] [w*]; UASp>mCD8-CIBN-NTEV-NICD-GFP/ Mat- alpha- tublin> Gal4; UASp> Cry2-CTEV-mCherry/ Mat- alpha- tublin> Gal4} were then crossed to any of their male siblings and their resultant embryos, named OptoNICD were used for experiments. These embryos were collected in the dark and fixed in the dark (photoactivation time (T=0)) or collected in the dark and photoactivated for 10, 20, 30, 60 or 120 minutes before fixation. We adjusted the collection times so the embryos would be fixed around the time they reached cephalic furrow formation or be within 30 minutes of this developmental time point. In other words, the longer the exposure time, the shorter the collection time. We also collected embryos that were for 120 minutes then aged in the dark for another 1 hour prior to fixation to study the effects of ectopic Notch activity on gastrulation progression. N^{+} embryos were photoactivated for 120 minutes prior to fixation or freezing for RNA collection.

Cloning:

We adapted the previously described system to develop a light-inducible variant of NICD[50] . Our system is composed of two distinct proteins. One is a cytosolic protein containing Cry2, mCherry, and the C-terminal portion of a split TEV protease (Cry2-mCherry-CTEV), while the other is a membrane tethered protein containing mCD8, CIBN, the complementary N-terminal portion of TEV protease, an ASLOV domain which masks a TEV cleavage sequence in the dark that precedes NICD, and GFP (mCD8-CIBN-NTEV-NICD-GFP). Upon illumination, Cry2 binds to CIBN, bringing the two components of the TEV protease together to reconstitute the functional protease and ASLOV undergoes a conformational change which exposes the TEV cleavage sequence. The TEV protease then cleaves its cleavage sequence liberating NICD from the membrane. NICD contains a nuclear localization sequence as the endogenous protein does so it translocates to the nucleus once it is liberated from the membrane.

We generated the Cry2-mCherry-CTEV cassette using PCR and Gibson assembly then used subcloned it into a pUASP-attb plasmid (DGRC # 1358). The resultant plasmid is named pUASP-attb-Cry2-CTEV-mCherry. The sequences were amplified from the following plasmids; pCRY2PHR-mCherryN1 (addgene# 26866) and FRB_SCF2_LD6_CTEV (addgene# 58879). The primers used were purchased from Sigma and are listed in Table S2. We also subcloned this cassette into a pAc5.1/V5-His A plasmid (Invitrogen #V4110-20) by cutting the cassette out of pUASP-attb-Cry2-CTEV-mCherry using NotI and XbaI (NEB #R3189S and #R0145S) and ligating to the linearized pAc5.1/V5-His A. The resultant plasmid was named pAC5.1-Cry2-mCherry-CTEV. Similarly, we subcloned the mCD8-CIBN-NTEV-NICD-GFP cassette, which was synthesized by Biobasic, into pUASP-attb and pAC5.1/V5-His A. The resultant plasmids were named: pUASP-attb-mcd8- CIBN-NTEV-NICD-GFP and pAC5.1-mcd8- CIBN-NTEV-NICD-GFP, respectively. We generated a pUASP-attb-mcd8- CIBN-NTEV-NICD without the GFP tag to allow us to preform experiments with other GFP tagged proteins. We also inserted these cassettes into pUAST-attb (DGRC #1419) for future use. The resultant plasmids were named: pUAST-attb-mCD8- CIBN-NTEV-NICD-GFP and pUAST-attb-Cry2-CTEV-mCherry.

S2 cell culture and Transient Transfection:

We used S2-DRSC cells (DGRC # 181) cells to test our Optogenetic tool prior to generating transgenic flylines. S2 cells were cultured at 25 ^{o}C in in Schneider's Insect Medium (Sigma-Aldrich Co. LLC #S0146) containing 10% heat inactivated fetal bovine serum (FBS), 500 ng/mL of insulin, and 100 µg/mL of Penicillin and Streptomycin. To transiently express our Optogenetic variant of NICD, we transfected S2 cells with pAC5.1-mcd8- CIBN-NTEV-NICD-GFP and pAC5.1-Cry2-mCherry-CTEV using the TransIT- Insect Reagent (Mirus, MIR #6104) according to manufacturer's recommendation. The media was changed 24 hours after transfection and cells were imaged between 36 and 48 hours after transfection. Cells were kept in the dark until imaging.

qRT-PCR:

For each genotype, 30 embryos were staged, and hand selected at cephalic furrow, prior to complete invagination of the ventral furrow. We used this developmental stage for several reasons; 1) the genes of interest are all expressed zygotically and maternal material has been degraded, 2) Notch signalling is active, 3) this stage represents early gastrulation and 4) limits variability, since ventral furrow invagination occurs over 15 mins in wildtype embryos. Embryos were flash frozen in liquid nitrogen and stored at -80 ^{o}C for no longer than 1 week before RNA extraction. Toal RNA was extracted using Trizol (Molecular Research Center Inc #TR 118) according to a previously published protocol[51]. 1ug of RNA was used to synthesize cDNA using (Bio rad kit) according to manufacturer's instructions. 1 ul of the synthesized cDNA was used in 10 ul qPCR reaction, assembled using SYBR green (bio rad kit) according to manufacturer's instructions. CFX maestro (machine) was used to read samples. Reactions were run in triplicates and negative controls, no-reverse transcriptase control and no-template controls were included in each run. Data was analyzed using the relative quantification method and normalization was preformed using RPS20 and RPL32 as housekeeping genes. Primers used for each target gene were purchased from Sigma and are listed in Table S3

Immunohistochemistry:

Embryos were collected on apple juice agar plates and fixed in 4% paraformaldehyde (Electron Microscopy Sciences, cat. 15710) and permeabilized in 1X PBT. Embryos were incubated to in 5% blocking buffer (5% skim milk in 1X PBT) for 20 minutes. Primary antibodies were diluted in 1% blocking buffer as follows; α-Twist (1:100) (kindly gifted by Eric Wieschaus), α-snail (1:100) (kindly gifted by Eric Wieschaus), α- Dorsal (1:20, DSHB), α-NECD (1:500, DSHB, C458.2H), and α-Delta (1:20, DSHB, C594.9B), added to the embryos and then incubated at 4 ^{o}C overnight. The next day, following three washes with 1% blocking buffer, the secondary antibodies were diluted as follows and added to the embryos, which were rocked at room temperature for 2 hours; α-mouse Alexa 568, α- mouse Alexa 488, and α-rat Alexa 568. Then the embryos were washed with 1% blocking buffer twice followed by a wash with 1X PBT, one wash with 1X PBS and then DAPI was diluted in 1X PBS and added to the embryos which were then rocked at room temperature for 20 minutes. Embryos were washed twice with 1X PBS and mounted in 50% glycerol/1X PBS. Cross-sections were cut by hand using a razor blade.

Fluorescent mRNA in situ hybridization:

Anti-sense probes were synthesized using the DIG and Biotin- RNA labelling kit (Roche, 11277073910 and 11685597910, respectively) according to manufacturer's recommendations. DNA templates were amplified using a forward primer and reverse primer containing a T7 RNA polymerase promoter sequence (5'-GTAATACGACTCACTATAG -3') from cDNA clones were obtained from DGRC (Table S4). A probe against *Sim* was labelled with Biotin and the probes against the mesodermal genes were labelled with DIG to allow us to preform dual- probe *in situ*

hybridizations. *In situs* were preformed according to previously described protocol with the following modifications[52]. The hybridization buffer was supplemented with 5% Dextran Sulfate (Sigma #D6001). Rather than using milk to block, we used 5% BSA for the initial blocking step and 1% for the washes in between antibodies and diluted the antibodies in 1% BSA. We incubated embryos in TSA buffer (Tyramide Cy3 AATBioquest Sciences 11065, in 0.003% H_2O_2) for 1 hour, except when probing for *wntD* and *Snail*, where a 2-hour incubation was necessary. The following antibodies were used in the following dilutions; monoclonal mouse α-biotin (1:300) (Jackson Immunoresearch, 200-472-211), Anti-Digoxigenin- POD Fab fragments (1:100) (Roche, 11207733910), and Goat α-mouse Alexa 488 (1:300) (Invitrogen A32723TR).

Microscopy:

All the imaging in this paper was preformed using an inverted Zeiss Axio Observer spinning disc confocal microscope equipped with a Yokogawa spinning disc head on a 20X objective (0.8 NA) for whole mount embryos or 40X oil immersion objective (1.4 NA) for S2 cells and embryo cross sections.

Image analysis:

Image analysis was preformed using ImageJ (RRID:SCR_002798). To quantify the number of cells in the mesoderm expressing Dorsal, Snail and Twist, we used line scans across the dorsoventral axis of embryos to generate a plot profile of the intensity across the embryo. We sampled 4 regions along the anterior-posterior axis per embryo and analyzed 3 or more embryos per genotype for each protein of interest. The specific numbers are stated in the corresponding figure captions. As expected, the plot profile generated a curve, where the peak region corresponds with the mesoderm, the area with the highest expression of these proteins. We then calculated the distance of the peak region of the plot profile and divided by the average cell size (5 microns) to determine the number of cells that were in the peak region. We automated this process using a python script and used it to analyze the outputs generated by ImageJ from the plots. Significance was determined using two-tailed T-tests to compare each genotype to wildtype and a p-value < 0.05 was considered significant.

Supplementary Table 1. Flylines used and generated in this paper.

Name in this paper	Source	Genotype
Wildtype (W1118)	Bloomington Stock Center (#3605)	w[1118]
Mat- alpha- tublin> Gal4	Bloomington Stock Center (#80361)	y[1] w[*]; P{matalpha4-GAL-VP16}67; P{matalpha4-GAL-VP16}15
UASp> Cry2-CTEV-mCherry	This paper	Chr3: UAS>Cry2-CTEV-mCherry / TM3
UASp>mCD8-CIBN-NTEV-NICD-GFP	This paper	Chr2: UAS> mCD8-CIBN-NTEV-NICD-GFP/ Cyo
UASp>OptoNICD	This paper	X: UAS> mCD8-CIBN-

		NTEV-NICD/ FM7i
Delta-TS	Kind gift by Eric Wieschaus	Chr3: DlRF/Dl6B37
Twi-	Bloomington Stock Center (#2381)	cn[1] twi[1] bw[1] speck[1]/CyO
OptoNICD	This paper	y[1] w[*]: UAS> mCD8-CIBN-NTEV-NICD-GFP; UAS>Cry2-CTEV-mCherry

Supplementary Table 2. Primer sequences used for cloning.

Primer name	**Sequence (5'-3')**
Cry2 forward	CACCATGAAGATGGACAAAAAGACT
mCherry reverse	GCATGGACGAGCTGTACAAG
CTEV forward	ATCTGGGTAAGATCTGGTATGTCTAG
CTEV reverse	CTTGTACAGCTCGTCCATGC
Cry2 forward with pUASP homology	GATCAGATCCGCGGCCGCCACCATGAAGATGGACAAAAAGACT
mCherry reverse with homology to CTEV	ATCTTACCCAGATCTTGTACAGCTCGTCCATGC
CTEV forward with homology to mCherry	CGAGCTGTACAAGATCTGGGTAAGATCTGGTATGTCTAG
CTEV reverse with pUASP homology	TTAACGTTAACGTTCGAGGTCGACTCTAGACTAATTCATGAGTTGAGTCGCTTCC

Supplementary Table 3. Primer sequences for qRT-PCR for mesodermal target genes.

Target gene	**5'-3' sequence**	**Source of the sequence**	**Annealing Temperature according to temperature gradient (^{o}C)**
Sim Forward	CAGACGCTGGACGGATTCATC	https://www.flyrnai.org/flyprimerbank	59.0
Sim Reverse	AGCGACAAAATGGCATTCATCT		
Asph Forward	GGCGTTCACATTACAAAGATGGG	https://www.flyrnai.org/flyprimerbank	59.0
Asph Reverse	CCGACAGAGGAGTGTCCAGAT		
Tinman Forward	AATCCCCACCAGTACCTCAAC	https://www.flyrnai.org/flyprimerbank	**61.4**
Tinman Reverse	GGCAAGAGTGGCGATAGGG		
Traf4 Forward	CTCAACGCCTGTAAGCACGAT	This paper	57.1
Traf4 Reverse	GTGCAGGTGTACTGGAGATGA		
Twist Forward	CCTCAACGACGCCTTCAAG	https://www.flyrnai.org/flyprimerbank	**57.0**
Twist Reverse	AAGTCAATGTATCTTGTGGCCAG		
Mes2 Forward	CGCCCACGTCAAGCTAATG	https://www.flyrnai.org/flyprimerbank	**55.7**
Mes2 Reverse	GCCCTTTCGTTCTCTGATGACA		
Mef2 Forward	ATATCACGCATCACCGATGAAC	https://www.flyrnai.org/flyprimerbank	**61.4**
Mef2 Reverse	GGCGTACTGGTACAGCTTGT		
Neurotactin Forward	AAATCTCGCCCAGGACTG	https://www.flyrnai.org/flyprimerbank	**57.1**
Neurotactin Reverse	GCTGTGGCTTCAGACTTG		
NetrinA Forward	TGGGGACAACGTAACCTTGAC	https://www.flyrnai.org/flyprimerbank	**65.0**

NetrinA Reverse	GTAGATCACCATCGAATCGGGA		
Heartless Forward	TGGGAGCCAGGAGTCAAAAC	https://www.flyrnai.org/flyprimerbank	61.4
Heartless Reverse	GAACTGACATTCACCGGCAA		
WntD Forward	AGACAACATGATTTTTGCCATC	This paper	65.0
WntD Reverse	GGGTGTACTGGTAGTAGCTCA		
String Forward	GAAAACAACTGCAGCATGGAT	https://www.flyrnai.org/flyprimerbank	**64.5**
String Reverse	CGACAGCTCCTCCTGGTC		
Stumps Forward	ACTTTCCTGAAGAACCACTTCG	https://www.flyrnai.org/flyprimerbank	**64.5**
Stumps Reverse	AAGGGACCATCGTCAATTTTGAT		
Snail Forward	AGCCGCAGGATCTATCCCT	https://www.flyrnai.org/flyprimerbank	60.6
Snail Reverse	GTGTTTTTGAAAGGTTCAGCACA		

Supplementary table 4. cDNA clones and primers used to amplify DNA templates to synthesize DIG and Biotin labeled antisense RNA probes for *in situ hybridizations*

Gene name	CG#	Clone#	Plasmid and antibiotic resistance	Primer sequences (5'-3')	DGRC RRID and stock number
sim	CG7771	RE54280	pFlc-1	Forward: AATCATGTACATCTCGG Reverse: AACTGCTCGAGCAGCTATTCG	RRID:DGRC_9345 Stock#: 9345
WntD (Wnt8)	CG8458	RE57705	PFLC-1 (ampR)	Forward: CATGATTTTTGCCATCACATTC Reverse: GCATTCCTGTTCCAGTGATCTT	RRID:DGRC_9748 Stock#: 9748

string	CG1395	LD47579	pOT2 (chlorR)	Forward: TCAACAAAATGAGTGGATCTCG Reverse: GATCAGCGAGTTTAGGCCACT	RRID:DGRC_2623 Stock #: 2623
netrinA	CG18657	RE11206	PFLC-1 (ampR)	Forward: CCAAAGTAATTGGTCGCGATAC Reverse: GCAGCGGCACTCCAGGT	RRID:DGRC_2623 Stock#: 2623
mes2	CG1110	SD09884	pOT2 (chlorR)	Forward: CATACTCATGCCAACGTCTCAT Reverse: ACTCAATATCCACCGAAAAACG	RRID:DGRC_3403 Stock #: 3403
Neurotactin	CG9704	LD22004	pOT2 (chlorR)	Forward: CCGACTTCGTTTCGTGTTTAGT Reverse: AGTCCTTCGATCTCAGACTTGC	RRID:DGRC_5736 Stock#: 5736
mef2	CG1429	LD08608	pBS SK - (ampR)	Forward: CAGCATCAACGGCAGCAACA Reverse: ACTATTACCGTAGGTCTG	RRID:DGRC_4409 Stock #: 4409
heartless (htl)	CG7223	LD32130	pOT2 (chlorR)	Forward: AGCACGGATTACTATCGGAAGA Reverse: TACACCACTTCTGCAGGTTGTC	RRID:DGRC_5217 Stock#: 5217

Stumps	CG31317	RE42507	pFlc-1 (ampR)	Forward: CATCCCAACGACACATATTGTAATC Reverse: TTCATGCTTAGCGGCATGC	RRID:DGRC_9029 Stock #: 9029

Figure Captions

Figure 1. NECD and Delta endocytosis in the mesoderm suggest Notch signalling is active in the mesoderm. A) a schematic of Notch signalling activation via the binding of the ligand, Delta, to the extracellular domain of the Notch receptor (NECD) on a neighbouring cell (signal receiving cell). This interaction leads to a series of cleavage events of the Notch receptor, separating the extracellular and intracellular domains of Notch. NECD and Delta are endocytosed into the signal sending cell, while the intracellular domain of Notch (NICD) is liberated from the plasma membrane and translocates to the nucleus, where it regulates gene expression. B) Cross sections of wildtype embryos at stage 4 showing the presence of Delta and NECD in mesoderm cells, indicating endocytosis and therefore Notch signalling activity. C) Target Notch genes that were expressed in the mesoderm, differentially expressed at nuclear cycle 14 and contained a Su(H) binding site include; *Asph*, *Tinman*, *Traf4*, *Twist, WntD*, *Stumps*, *String Heartless*, *NetrinA*, *Neurotactin*, *mir-1*, *Mes2*, and *Mef2*. Only the binding sites preceding the 5'UTR are shown and the distances from the first base pair of the 5'UTR are labeled. Su(H) sites are found upstream of the 5'UTR of all transcripts of the genes above except for *Asph*, and *Twist*.

Figure 2. Expression of mesodermal genes in wildtype and loss of function delta mutant embryos show that Notch signalling is necessary for the expression of many mesodermal genes. A-C) fluorescent mRNA *in situ* hybridizations against *sim* (green)and mesodermal genes (purple) in wildtype and Delta mutant embryos at cephalic furrow (stage 5-6). A) shows examples of genes whose expression was significantly reduced in Delta mutants compared to their wildtype counterparts; *Stumps, String,* and *Mef2*. B) shows expression of the two genes whose expression was upregulated in Delta mutants; *Heartless* and *WntD.* C) Expression of *NetrinA* was unchanged in Delta mutants. D-F) Normalized relative expression of mesodermal genes and *sim* in wildtype and Delta mutant embryos at cephalic furrow (stage 5-6). D) Expression of *Asph*, *Mef2*, *Mes2*, *Neurotactin*, *String*, *Stumps*, *Tinman*, *Traf4*, and *Twist* is significantly reduced in Delta mutants compared to stage matched wildtype embryos. E) Expression of *Heartless* and *WntD* is significantly increased in Delta mutants, while F) the expression of *NetrinA* was not significantly changed. Independent two-tailed T-tests were preformed for each gene to compare expression in Delta mutants to that in wildtype embryos. '*' indicates statistical significance determined by a p-value less than 0.05. Error bars represent the standard error of the mean.

Figure 3. Development of Optogenetic NICD reveals competency of mesodermal cells to express a Notch target gene, *sim.* A) Schematic of the mechanism of the Optogenetic variant of NICD (Opto-NICD) that we developed which is described in detail in the text. B) S2 cells were transiently transfected with Opto-NICD before and after photoactivation for 1 hour. Prior to photoactivation, NICD-GFP is excluded from the nucleus, while after photoactivation, NICD is seen in the nucleus. C) *sim* (green) expression in embryos expressing Opto-NICD that have been not photoactivated, photoactivated for 10, 20, 30, 60

and 120 minutes visualized by fluorescent mRNA *in situ* hybridization. Expression of *sim* is incrementally expanded into lateral regions of Opto-NICD embryos photoactivated for 10,20 and 30 minutes (stage4 embryos shown, prior to cephalic furrow formation). *Sim* expression is observed in the regions of mesoderm of Opto-NICD embryos photoactivated for 60 and 120 minutes (stage 5-6 embryos shown) D) Normalized Relative expression of *Sim* of wildtype and Opto-NICD embryos photoactivated for different durations. Independent two-tailed T-tests were preformed for each gene to compare expression in Delta mutants to that in wildtype embryos. '*' indicates statistical significance determined by a p-value less than 0.05. Error bars represent the standard error of the mean. E) Brightfield images of wildtype and Opto-NICD (N+) embryos (photoactivated for 2 hours) at different stages of gastrulation. Morphological defects along the anterior-posterior axis can be observed in N+ embryos during early gastrulation and complete breakdown is observed during later stages.

Figure 4. Expression of mesodermal genes in wildtype and gain of function Notch mutant (Opto-Notch) embryos shows that Notch supresses most mesodermal genes and the sufficiency of Notch to drive overexpression of *WntD* and *String*. A,C,E) fluorescent mRNA *in situ* hybridizations against *sim* (green)and mesodermal genes (purple) in wildtype and N+ embryos (Opto-NICD embryos photoactivated for 2 hours) at cephalic furrow (stage 5-6). A) shows examples of genes whose expression was significantly reduced in N^+ embryos (Opto-Notch embryos photoactivated for 2 hours) compared to their wildtype counterparts; *Stumps, NetrinA,* and *Heartless*. C& E) shows expression of the two genes whose expression was upregulated in Delta mutants; *String* and *WntD.* Their expression expands laterally into the ectoderm of N+ embryos. B,D,F) Normalized relative expression of mesodermal genes in wildtype and N+ embryos at cephalic furrow (stage 5-6). B) Expression of *Asph*, *Mef2*, *Mes2*, *Neurotactin*, *NetrinA*, *Stumps*, *Tinman*, *Heartless*, and *Traf4* is significantly reduced in N+ compared to stage matched wildtype embryos. D) Expression of *String* is significantly increased in N+ embryos compared to wildtype embryos. F) Expression of *WntD* is significantly increased to different levels in Opto-NICD embryos photoactivated for different durations of time. Independent two-tailed T-tests were preformed for each gene to compare expression in Delta mutants to that in wildtype embryos. '*' indicates statistical significance determined by a p-value less than 0.05. Error bars represent the standard error of the mean.

Figure 5. Twist and Snail protein and mRNA expression in wildtype and Notch gain-of-function and loss-of-function mutant embryos. A) Twist protein expression during cellularization, early and late gastrulation in wildtype, loss-of-function (D^-) and gain-of-function Notch mutants (N^+, Opto-Notch embryos photoactivated for 2 hours prior to fixation). B) Number of Twist positive cells in cellular blastoderms (WT: n= 3, D^-: n=4, N^+: n=4). Error bars represent standard deviation. C) Normalized relative mRNA expression of *twist,* n= 30 embryos at cephalic furrow formation in each genotype. Error bars represent SEM. D) Snail protein expression during cellularization, early and late gastrulation in wildtype, D^-, and N^+ mutant embryos. E) Number of Snail positive cells in cellular blastoderms (WT: n= 6, D^-: n=5, N^+: n=3). Error bars represent standard deviation. F) Normalized relative mRNA expression of *snail*, n= 30 embryos at cephalic furrow formation in each genotype. Error bars represent SEM. Statistical significance is denoted by '*' (a p-value <0.05) determined from a two-tailed t-Test comparing wildtype embryos to Delta mutants and wildtypes to N+ mutants.

Figure 6. Expression of Dorsal in wildtype and Notch gain-of-function and loss-of-function mutant embryos. A) Dorsal protein expression in cellular blastoderm embryos. N^+ are Opto-Notch embryos photoactivated for 2 hours prior to fixation. B) Signal plots of line scans of embryos from each genotype.

C) The number of cells in the mesoderm determined using the peak region from the line scan plots. Statistical significance is denoted by '*' (a p-value <0.05) determined from a two-tailed t-Test comparing wildtype embryos (n=3) to each genotype: Delta mutants (n=3), N+ mutants that had a higher level of Dl expression (n=3), and N^+ mutants with a very low level of Dl signal (n=3). Error bars represent standard deviation.

Supplementary figure 1. Bright field images of wildtype and mutant embryos at germband extension (stage 9-11). Loss-of-function Twist mutants have similar morphological defects as gain-of-function and loss of function mutants in the Notch signalling pathway such as aberrant invaginations along the AP axis and the overall twisted body phenotype.

Supplementary figure 2. Expression of mesodermal genes in wildtype and Opto-NICD embryos following photoactivation for short durations. Normalized relative mRNA expression of mesodermal genes, n= 30 embryos at cephalic furrow formation in each genotype. Error bars represent SEM. Statistical significance is denoted by '*' (a p-value <0.05) determined from a two-tailed t-Test comparing wildtype embryos to Delta mutants and wildtypes to N+ mutants. A) shows expression in wildtype (blue bars), Opto-NICD embryos photoactivated for 10 minutes (red bars) and 1 hour (green bars). B) Shows *NetrinA* expression in wildtype (blue bar), Opto-NICD embryos photoactivated for 10 minutes (red bar), 20 minutes (green bar), 30 minutes (purple bar), 1 hour (orange bar), and 2 hours (black bar).

References:

(1) Bray, S. J. (2016). Notch signalling in context. Nature reviews Molecular cell biology, 17(11), 722.
(2) Leptin, M. (1999). Gastrulation in *Drosophila*: the logic and the cellular mechanisms. The EMBO journal, 18(12), 3187-3192.
(3) Farrell, J. A., & O'Farrell, P. H. (2014). From egg to gastrula: how the cell cycle is remodeled during the Drosophila mid-blastula transition. Annual review of genetics, 48, 269-294.
(4) Leptin, M. (1995). Drosophila gastrulation: from pattern formation to morphogenesis. Annual review of cell and developmental biology, 11(1), 189-212.
(5) St Johnston D and Nüsslein-Volhard C (1992) The origin of pattern and polarity in the Drosophila embryo. Cell, 68, 201–219.
(6) Tautz, D. (1988). Regulation of the Drosophila segmentation gene hunchback by two maternal morphogenetic centres. Nature, 332(6161), 281-284.
(7) Tautz, D., & Pfeifle, C. (1989). A non-radioactive in situ hybridization method for the localization of specific RNAs in Drosophila embryos reveals translational control of the segmentation gene hunchback. Chromosoma, 98(2), 81-85.
(8) Wilson, R., Vogelsang, E., & Leptin, M. (2005). FGF signalling and the mechanism of mesoderm spreading in Drosophila embryos.
(9) Joutel, A., & Tournier-Lasserve, E. (1998). Notch signalling pathway and human diseases. In Seminars in cell & developmental biology (Vol. 9, No. 6, pp. 619-625). Academic Press.

(10) Lehmann, R., Jiménez, F., Dietrich, U., & Campos-Ortega, J. A. (1983). On the phenotype and development of mutants of early neurogenesis in *Drosophila melanogaster*. Wilhelm Roux's archives of developmental biology, 192(2), 62-74.
(11) De Renzis, S., Yu, J., Zinzen, R., & Wieschaus, E. (2006). Dorsal-ventral pattern of Delta trafficking is established by a Snail-Tom-Neuralized pathway. Developmental cell, 10(2), 257-264.
(12) Pavlopoulos, E., Pitsouli, C., Klueg, K. M., Muskavitch, M. A., Moschonas, N. K., & Delidakis, C. (2001). neuralized Encodes a peripheral membrane protein involved in delta signaling and endocytosis. Developmental cell, 1(6), 807-816.
(13) Lai, E. C., Deblandre, G. A., Kintner, C., & Rubin, G. M. (2001). Drosophila neuralized is a ubiquitin ligase that promotes the internalization and degradation of delta. Developmental cell, 1(6), 783-794.
(14) Morel, V., & Schweisguth, F. (2000). Repression by suppressor of hairless and activation by Notch are required to define a single row of single-minded expressing cells in the Drosophila embryo. Genes & development, 14(3), 377-388.
(15) Hemavathy, K., Meng, X., & Ip, Y. T. (1997). Differential regulation of gastrulation and neuroectodermal gene expression by Snail in the Drosophila embryo. Development, 124(19), 3683-3691.
(16) Brown, J.B., Boley, N., Eisman, R., May, G.E., Stoiber, M.H., Duff, M.O., Booth, B.W., Wen, J., Park, S., Suzuki, A.M., Wan, K.H., Yu, C., Zhang, D., Carlson, J.W., Cherbas, L., Eads, B.D., Miller, D., Mockaitis, K., Roberts, J., Davis, C.A., Frise, E., Hammonds, A.S., Olson, S., Shenker, S., Sturgill, D., Samsonova, A.A., Weiszmann, R., Robinson, G., Hernandez, J., Andrews, J., Bickel, P.J., Carninci, P., Cherbas, P., Gingeras, T.R., Hoskins, R.A., Kaufman, T.C., Lai, E.C., Oliver, B., Perrimon, N., Graveley, B.R., Celniker, S.E. (2014.8.27). modENCODE RNA-Seq data remapped to BDGP Release 6 genome assembly.
(17) Stathopoulos, A., Van Drenth, M., Erives, A., Markstein, M., & Levine, M. (2002). Whole-genome analysis of dorsal-ventral patterning in the *Drosophila* embryo. Cell, 111(5), 687-701.
(18) Ozdemir, A., Ma, L., White, K. P., & Stathopoulos, A. (2014). Su (H)-mediated repression positions gene boundaries along the dorsal-ventral axis of *Drosophila* embryos. Developmental cell, 31(1), 100-113.
(19) Leptin, M. (1991). *twist* and *snail* as positive and negative regulators during *Drosophila* mesoderm development. Genes & development, 5(9), 1568-1576.
(20) Roth S, Stein D. NUsslein-Volhard C. 1989. A gradient of nuclear localization of the dorsal protein determines dorsoventral pattern in the Drosophila embryo. Cell 59: 1189-202.
(21) Steward R. 1989. Relocalization of the dorsal protein from the cytoplasm to the nucleus correlates with its function. Cell 59: 117988.
(22) Govind, S., Brennan, L., & Steward, R. (1993). Homeostatic balance between dorsal and cactus proteins in the Drosophila embryo. Development, 117(1), 135-148.
(23) Lemaitre, B., Meister, M., Govind, S., Georgel, P., Steward, R., Reichhart, J.M., Hoffmann, J.A. (1995). Functional analysis and regulation of nuclear import of dorsal during the immune response in Drosophila. EMBO J. 14(3): 536--545.
(24) Roth, S., Hiromi, Y., Godt, D. and Nüsslein-Volhard, C. (1991). cactus, a maternal gene required for proper formation of the dorsoventral morphogen gradient in Drosophila embryos. Development 112, 371-388.

(25) Ganguly, A., Jiang, J., & Ip, Y. T. (2005). Drosophila WntD is a target and an inhibitor of the Dorsal/Twist/Snail network in the gastrulating embryo.
(26) Espinosa, L., Cathelin, S., D'Altri, T., Trimarchi, T., Statnikov, A., Guiu, J., ... & Bigas, A. (2010). The Notch/Hes1 pathway sustains NF-κB activation through CYLD repression in T cell leukemia. Cancer cell, 18(3), 268-281.
(27) Park, M., Yaich, L. E., & Bodmer, R. (1998). Mesodermal cell fate decisions in Drosophila are under the control of the lineage genes numb, Notch, and sanpodo. Mechanisms of development, 75(1-2), 117-126.
(28) Campos□Ortega, J. A. (1993). Mechanisms of early neurogenesis in Drosophila melanogaster. Journal of neurobiology, 24(10), 1305-1327.
(29) Tapanes-Castillo, A., & Baylies, M. K. (2004). Notch signaling patterns Drosophila mesodermal segments by regulating the bHLH transcription factor twist
(30) Krejčí, A., Bernard, F., Housden, B. E., Collins, S., & Bray, S. J. (2009). Direct response to Notch activation: signaling crosstalk and incoherent logic. Science signaling, 2(55), ra1-ra1.
(31) Sandmann, T., Girardot, C., Brehme, M., Tongprasit, W., Stolc, V., & Furlong, E. E. (2007). A core transcriptional network for early mesoderm development in Drosophila melanogaster. Genes & development, 21(4), 436-449.
(32) Yin, Z., Xu, X. L., & Frasch, M. (1997). Regulation of the twist target gene tinman by modular cis-regulatory elements during early mesoderm development. Development, 124(24), 4971-4982.
(33) Zimmermann, G., Furlong, E. E., Suyama, K., & Scott, M. P. (2006). Mes2, a MADF□containing transcription factor essential for Drosophila development. Developmental dynamics: an official publication of the American Association of Anatomists, 235(12), 3387-3395.
(34) Furlong, E. E., Andersen, E. C., Null, B., White, K. P., & Scott, M. P. (2001). Patterns of gene expression during Drosophila mesoderm development. Science, 293(5535), 1629-1633.
(35) Taylor, M. V., Beatty, K. E., Hunter, H. K., & Baylies, M. K. (1995). Drosophila MEF2 is regulated by twist and is expressed in both the primordia and differentiated cells of the embryonic somatic, visceral and heart musculature. Mechanisms of development, 50(1), 29-41.
(36) Gajewski, K., Kim, Y., Choi, C. Y., & Schulz, R. A. (1998). Combinatorial control of Drosophila mef2 gene expression in cardiac and somatic muscle cell lineages. Development genes and evolution, 208, 382-392.
(37) Mathew, S. J., Rembold, M., & Leptin, M. (2011). Role for Traf4 in polarizing adherens junctions as a prerequisite for efficient cell shape changes. Molecular and cellular biology, 31(24), 4978-4993.
(38) De la Escalera, S., Bockamp, E. O., Moya, F., Piovant, M., & Jimenez, F. (1990). Characterization and gene cloning of neurotactin, a Drosophila transmembrane protein related to cholinesterases. The EMBO journal, 9(11), 3593-3601.
(39) Sun, J., Macabenta, F., Akos, Z., & Stathopoulos, A. (2020). Collective migrations of Drosophila embryonic trunk and caudal mesoderm-derived muscle precursor cells. Genetics, 215(2), 297-322.
(40) Dawes-Hoang, R. E., Parmar, K. M., Christiansen, A. E., Phelps, C. B., Brand, A. H., & Wieschaus, E. F. (2005). Folded gastrulation, cell shape change and the control of myosin localization.

(41) Mortimer, N. T., & Moberg, K. H. (2013). The archipelago ubiquitin ligase subunit acts in target tissue to restrict tracheal terminal cell branching and hypoxic-induced gene expression. PLoS genetics, 9(2), e1003314.
(42) Kopan, R., & Ilagan, M. X. G. (2009). The canonical Notch signaling pathway: unfolding the activation mechanism. Cell, 137(2), 216-233.
(43) Edgar, B. A., & O'Farrell, P. H. (1989). Genetic control of cell division patterns in the Drosophila embryo. Cell, 57(1), 177-187.
(44) Lehman, D. A., Patterson, B., Johnston, L. A., Balzer, T., Britton, J. S., Saint, R., & Edgar, B. A. (1999). Cis-regulatory elements of the mitotic regulator, string/Cdc25. Development, 126(9), 1793-1803.
(45) Rahimi, N., Averbukh, I., Haskel-Ittah, M., Degani, N., Schejter, E. D., Barkai, N., & Shilo, B. Z. (2016). A WntD-dependent integral feedback loop attenuates variability in Drosophila Toll signaling. Developmental cell, 36(4), 401-414.
(46) Feng, J., Liu, T., & Zhang, Y. (2011). Using MACS to identify peaks from ChIP□Seq data. Current protocols in bioinformatics, 34(1), 2-14.
(47) Quinlan, A. R., & Hall, I. M. (2010). BEDTools: a flexible suite of utilities for comparing genomic features. Bioinformatics, 26(6), 841-842.
(48) Backhaus, B., Sulkowski, E., Schlote, F.W. (1984). A semi-synthetic, general-purpose medium for Drosophila melanogaster. D. I. S. 60(): 210--212.
(49) Parody, T. R., & Muskavitch, M. A. (1993). The pleiotropic function of Delta during postembryonic development of Drosophila melanogaster. Genetics, 135(2), 527-539.
(50) Lee, D., Creed, M., Jung, K., Stefanelli, T., Wendler, D. J., Oh, W. C., ... & Kwon, H. B. (2017). Temporally precise labeling and control of neuromodulatory circuits in the mammalian brain. Nature methods, 14(5), 495-503.
(51) Bogart, K., & Andrews, J. (2006). CGB Technical Report 2006-10. Extraction.
(52) Wilk, R., Murthy, S. U., Yan, H., & Krause, H. M. (2010). In situ hybridization: fruit fly embryos and tissues. Current Protocols Essential Laboratory Techniques, 4(1), 9-3.

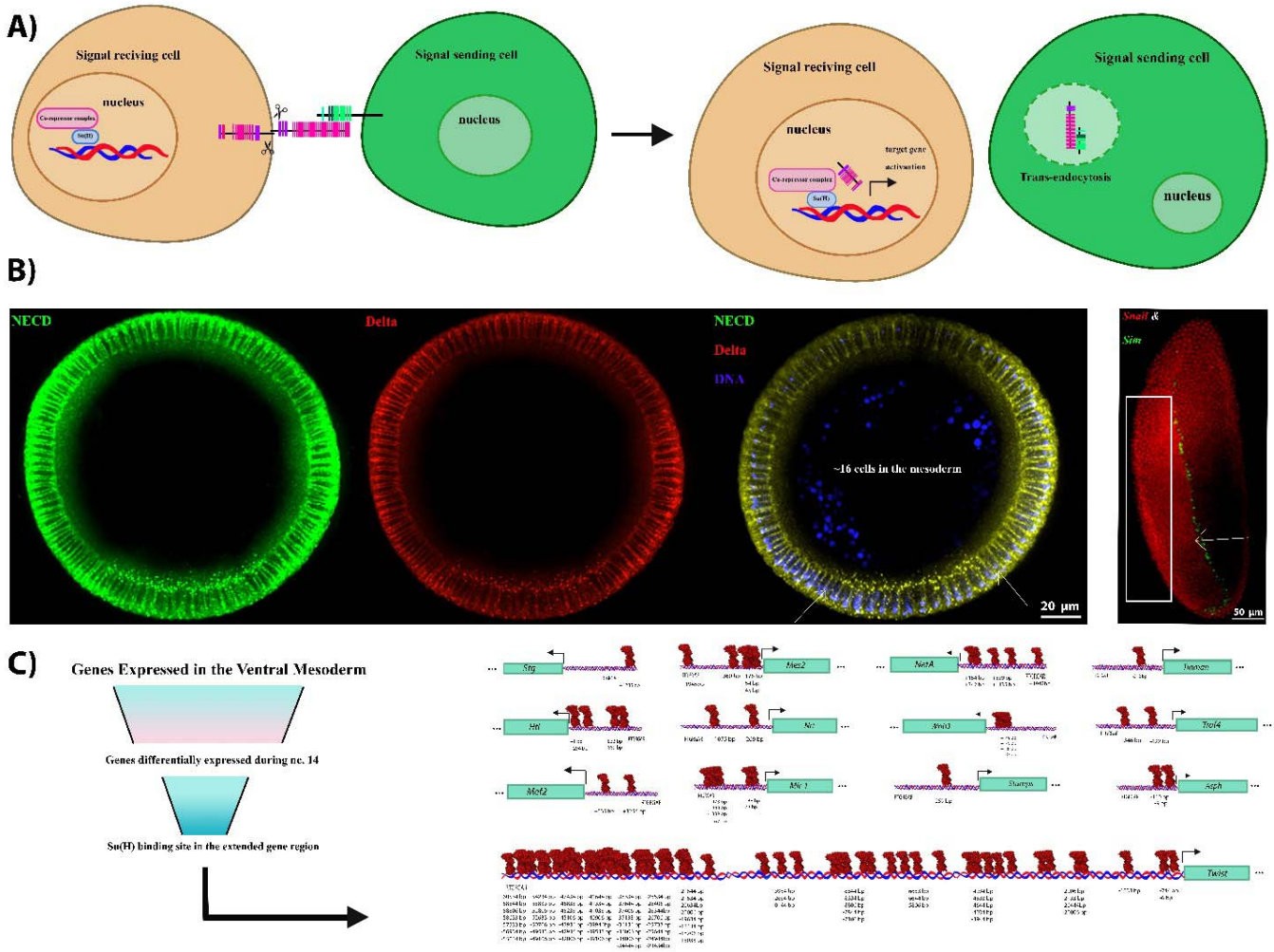

Figure 1. NECD and Delta endocytosis in the mesoderm suggest Notch signalling is active in the mesoderm. A) a schematic of Notch signalling activation via the binding of the ligand, Delta, to the extracellular domain of the Notch receptor (NECD) on a neighbouring cell (signal receiving cell). This interaction leads to a series of cleavage events of the Notch receptor, separating the extracellular and intracellular domains of Notch. NECD and Delta are endocytosed into the signal sending cell, while the intracellular domain of Notch (NICD) is liberated from the plasma membrane and translocates to the nucleus, where it regulates gene expression. B) Cross sections of wildtype embryos at stage 4 showing the presence of Delta and NECD in mesoderm cells, indicating endocytosis and therefore Notch signalling activity. C) Target Notch genes that were expressed in the mesoderm, differentially expressed at nuclear cycle 14 and contained a Su(H) binding site include; *Asph*, *Tinman*, *Traf4*, *Twist*, *WntD*, *Stumps*, *String Heartless*, *NetrinA*, *Neurotactin*, *mir-1*, *Mes2*, and *Mef2*. Only the binding sites preceding the 5'UTR are shown and the distances from the first base pair of the 5'UTR are labeled. Su(H) sites are found upstream of the 5'UTR of all transcripts of the genes above except for *Asph*, and *Twist*.

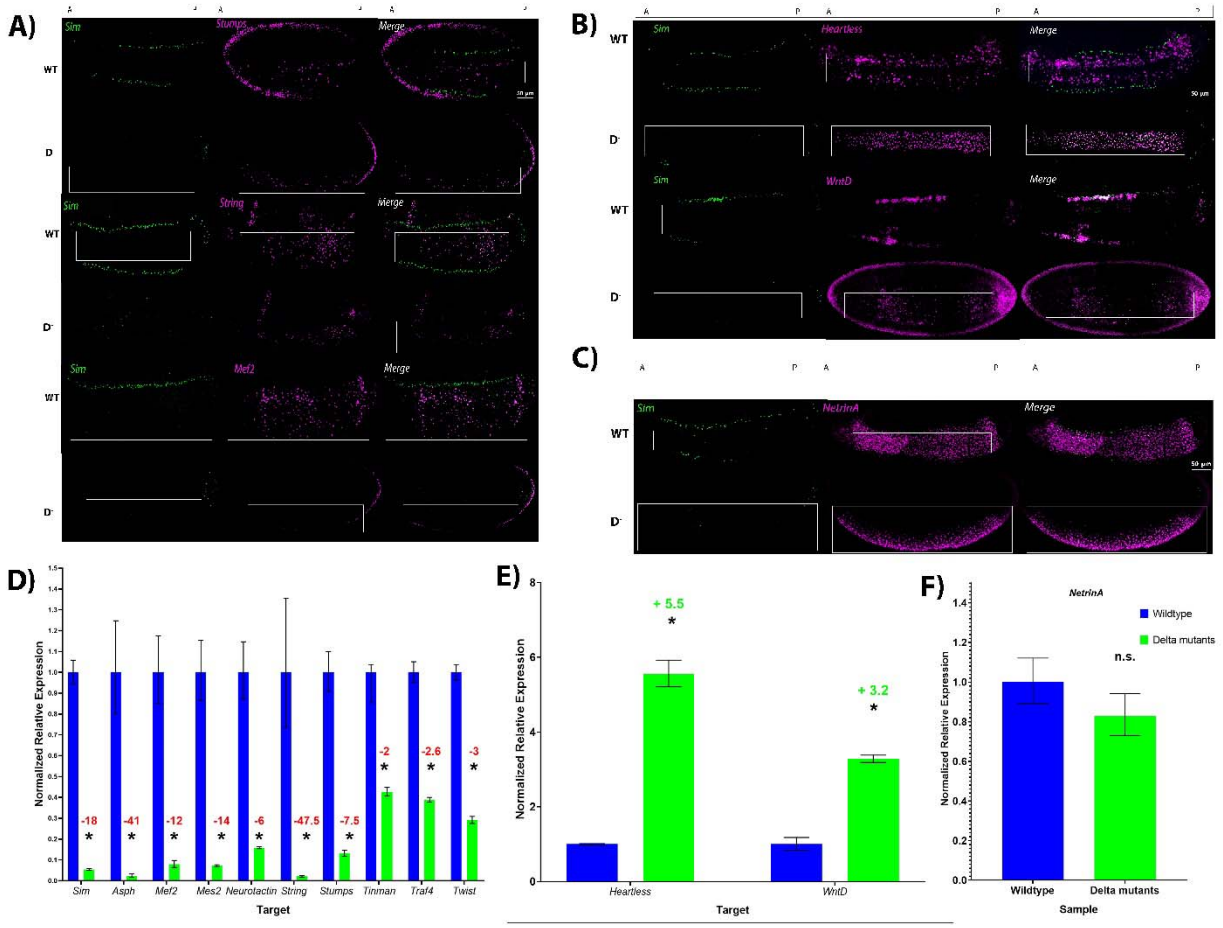

Figure 2. Expression of mesodermal genes in wildtype and loss of function delta mutant embryos show that Notch signalling is necessary for the expression of many mesodermal genes. A-C) fluorescent mRNA *in situ* hybridizations against *sim* (green)and mesodermal genes (purple) in wildtype and Delta mutant embryos at cephalic furrow (stage 5-6). A) shows examples of genes whose expression was significantly reduced in Delta mutants compared to their wildtype counterparts; *Stumps, String,* and *Mef2*. B) shows expression of the two genes whose expression was upregulated in Delta mutants; *Heartless* and *WntD.* C) Expression of *NetrinA* was unchanged in Delta mutants. D-F) Normalized relative expression of mesodermal genes and *sim* in wildtype and Delta mutant embryos at cephalic furrow (stage 5-6). D) Expression of *Asph*, *Mef2*, *Mes2*, *Neurotactin*, *String*, *Stumps*, *Tinman*, *Traf4*, and *Twist* is significantly reduced in Delta mutants compared to stage matched wildtype embryos. E) Expression of *Heartless* and *WntD* is significantly increased in Delta mutants, while F) the expression of *NetrinA* was not significantly changed. Independent two-tailed T-tests were preformed for each gene to compare expression in Delta mutants to that in wildtype embryos. '*' indicates statistical significance determined by a p-value less than 0.05. Error bars represent the standard error of the mean.

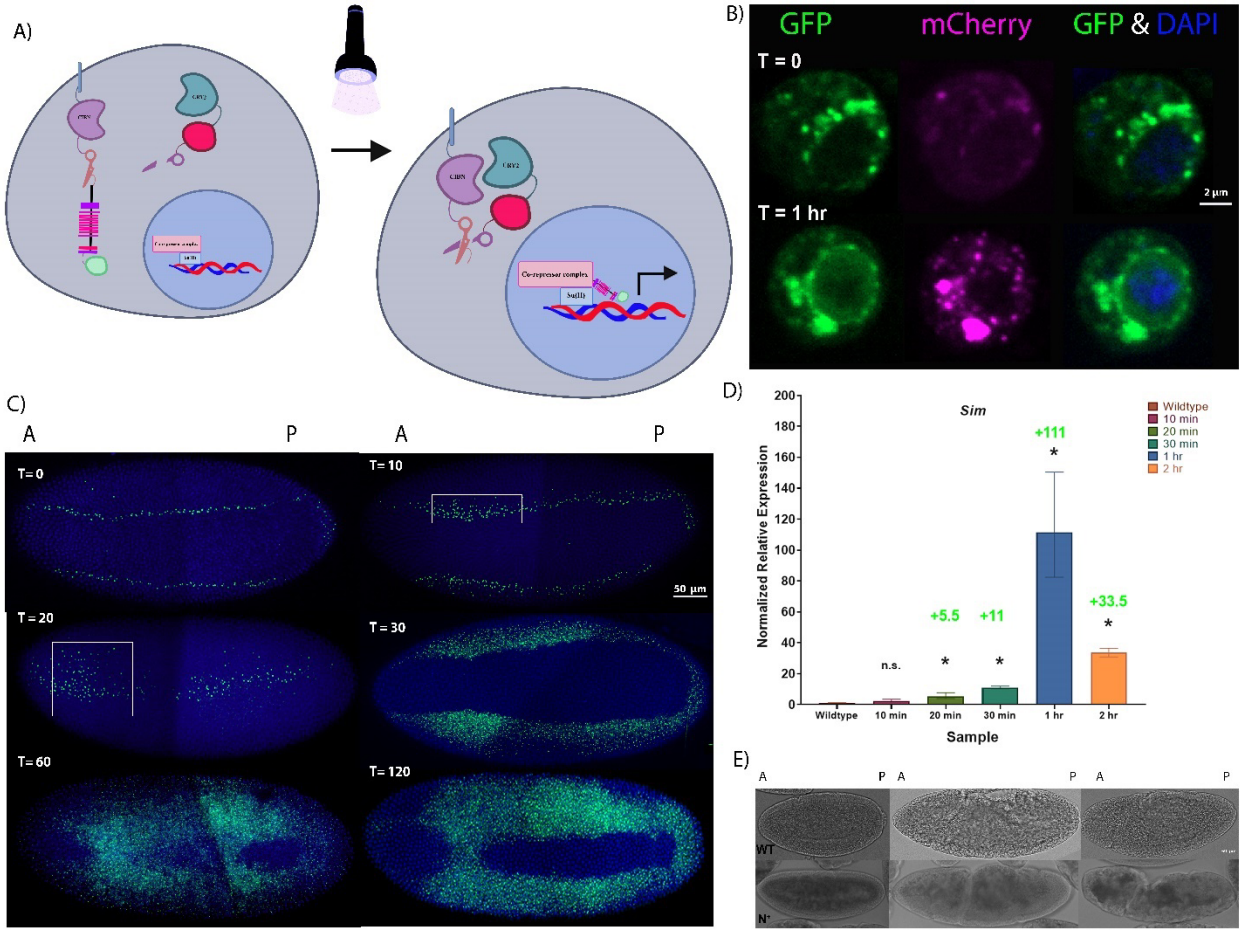

Figure 3. Development of Optogenetic NICD reveals competency of mesodermal cells to express a Notch target gene, *sim*. A) Schematic of the mechanism of the Optogenetic variant of NICD (Opto-NICD) that we developed which is described in detail in the text. B) S2 cells were transiently transfected with Opto-NICD before and after photoactivation for 1 hour. Prior to photoactivation, NICD-GFP is excluded from the nucleus, while after photoactivation, NICD is seen in the nucleus. C) *sim* (green) expression in embryos expressing Opto-NICD that have been not photoactivated, photoactivated for 10, 20, 30, 60 and 120 minutes visualized by fluorescent mRNA *in situ* hybridization. Expression of *sim* is incrementally expanded into lateral regions of Opto-NICD embryos photoactivated for 10,20 and 30 minutes (stage4 embryos shown, prior to cephalic furrow formation). *Sim* expression is observed in the regions of mesoderm of Opto-NICD embryos photoactivated for 60 and 120 minutes (stage 5-6 embryos shown) D) Normalized Relative expression of *Sim* of wildtype and Opto-NICD embryos photoactivated for different durations. Independent two-tailed T-tests were preformed for each gene to compare expression in Delta mutants to that in wildtype embryos. '*' indicates statistical significance determined by a p-value less than 0.05. Error bars represent the standard error of the mean. E) Brightfield images of wildtype and Opto-NICD (N+) embryos (photoactivated for 2 hours) at different stages of gastrulation. Morphological defects along the anterior-posterior axis can be observed in N+ embryos during early gastrulation and complete breakdown is observed during later stages.

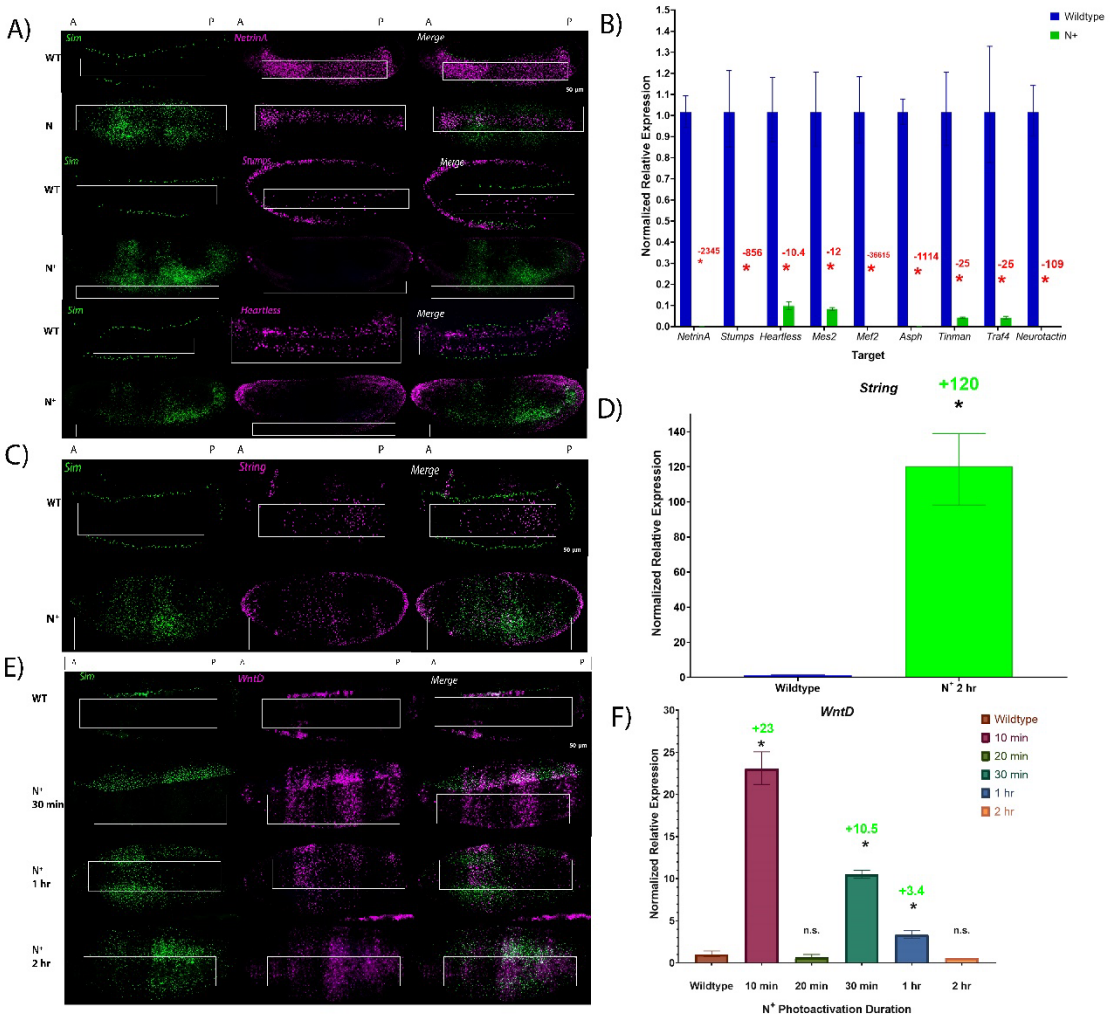

Figure 4. Expression of mesodermal genes in wildtype and gain of function Notch mutant (Opto-Notch) embryos shows that Notch supresses most mesodermal genes and the sufficiency of Notch to drive overexpression of *WntD* and *String*. A,C,E) fluorescent mRNA *in situ* hybridizations against *sim* (green)and mesodermal genes (purple) in wildtype and N+ embryos (Opto-NICD embryos photoactivated for 2 hours) at cephalic furrow (stage 5-6). A) shows examples of genes whose expression was significantly reduced in N^+ embryos (Opto-Notch embryos photoactivated for 2 hours) compared to their wildtype counterparts; *Stumps*, *NetrinA,* and *Heartless*. C& E) shows expression of the two genes whose expression was upregulated in Delta mutants; *String* and *WntD.* Their expression expands laterally into the ectoderm of N+ embryos. B,D,F) Normalized relative expression of mesodermal genes in wildtype and N+ embryos at cephalic furrow (stage 5-6). B) Expression of *Asph*, *Mef2*, *Mes2*, *Neurotactin*, *NetrinA*, *Stumps*, *Tinman*, *Heartless*, and *Traf4* is significantly reduced in N+ compared to stage matched wildtype embryos. D) Expression of *String* is significantly increased in N+ embryos compared to wildtype embryos. F) Expression of *WntD* is significantly increased to different levels in Opto-NICD embryos photoactivated for different durations of time. Independent two-tailed T-tests were preformed for each gene to compare expression in Delta mutants to that in wildtype embryos. '*' indicates statistical significance determined by a p-value less than 0.05. Error bars represent the standard error of the mean.

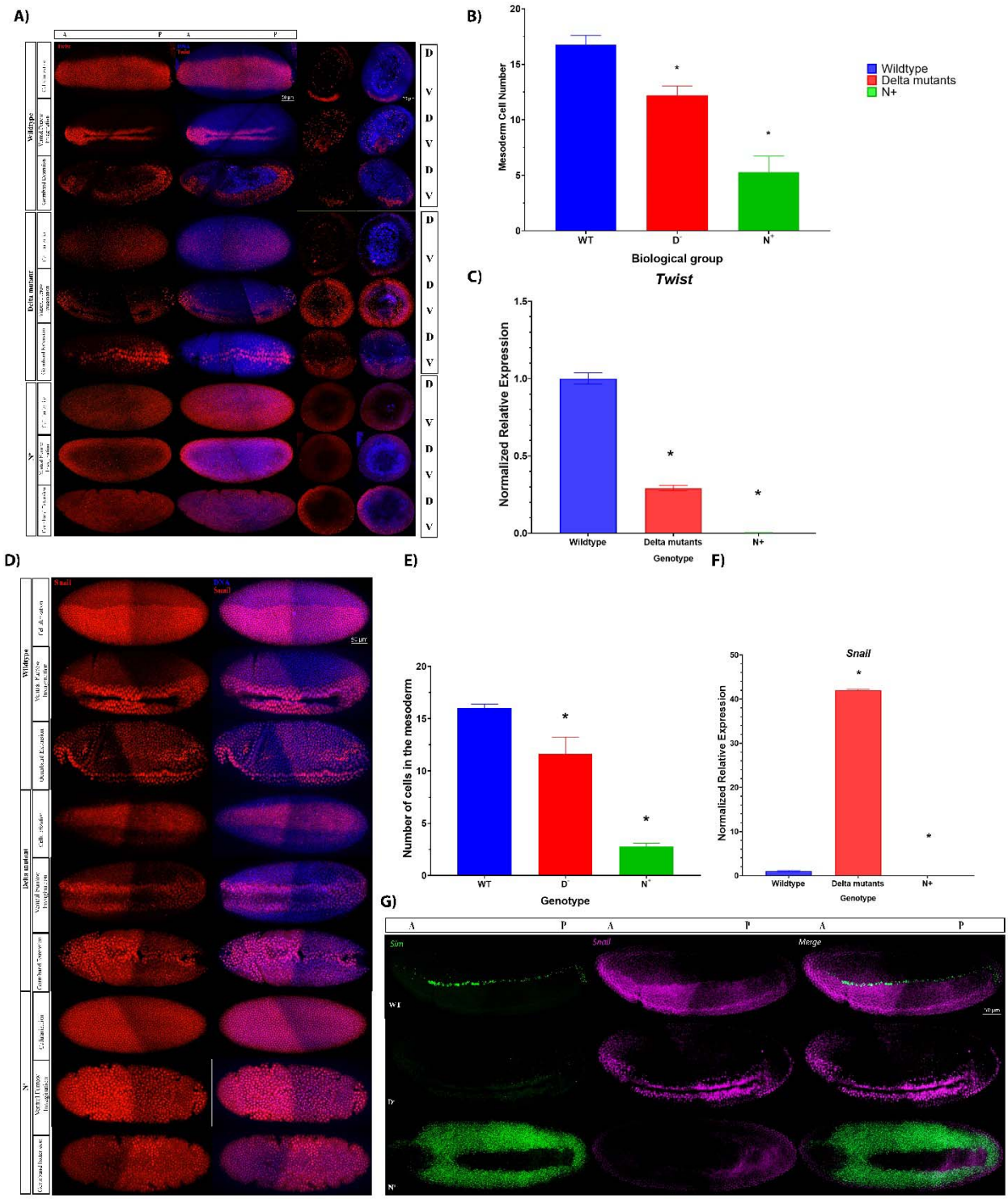

Figure 5. Twist and Snail protein and mRNA expression in wildtype and Notch gain-of-function and loss-of-function mutant embryos. A) Twist protein expression during cellularization, early and late gastrulation in wildtype, loss-of-function (D^-) and gain-of-function Notch mutants (N^+, Opto-Notch

embryos photoactivated for 2 hours prior to fixation). B) Number of Twist positive cells in cellular blastoderms (WT: n= 3, D^-: n=4, N^+: n=4). Error bars represent standard deviation. C) Normalized relative mRNA expression of *twist,* n= 30 embryos at cephalic furrow formation in each genotype. Error bars represent SEM. D) Snail protein expression during cellularization, early and late gastrulation in wildtype, D^-, and N^+ mutant embryos. E) Number of Snail positive cells in cellular blastoderms (WT: n= 6, D^-: n=5, N^+: n=3). Error bars represent standard deviation. F) Normalized relative mRNA expression of *snail*, n= 30 embryos at cephalic furrow formation in each genotype. Error bars represent SEM. Statistical significance is denoted by '*' (a p-value <0.05) determined from a two-tailed t-Test comparing wildtype embryos to Delta mutants and wildtypes to N+ mutants.

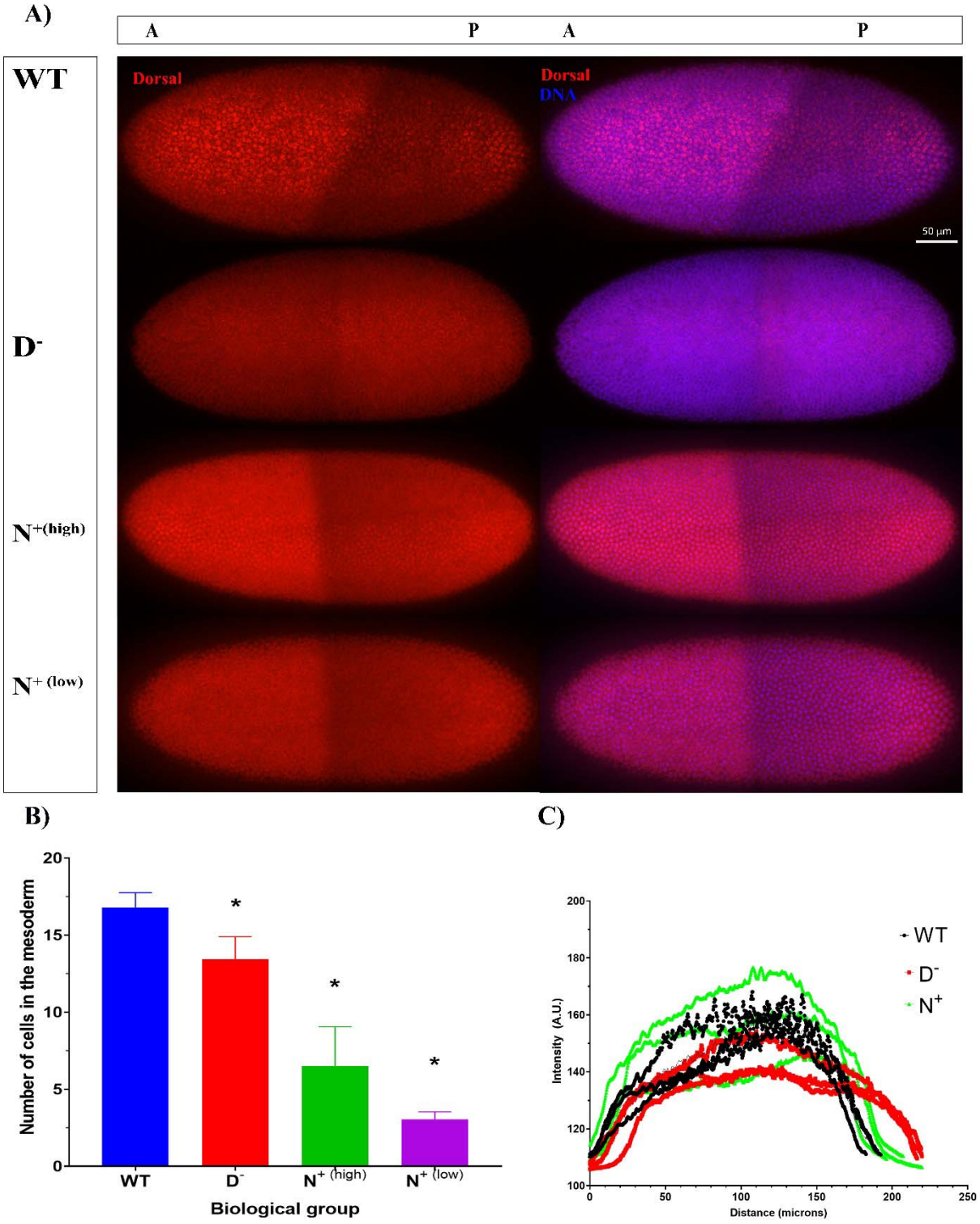

Figure 6. Expression of Dorsal in wildtype and Notch gain-of-function and loss-of-function mutant embryos. A) Dorsal protein expression in cellular blastoderm embryos. N^+ are Opto-Notch embryos

photoactivated for 2 hours prior to fixation. B) Signal plots of line scans of embryos from each genotype. C) The number of cells in the mesoderm determined using the peak region from the line scan plots. Statistical significance is denoted by '*' (a p-value <0.05) determined from a two-tailed t-Test comparing wildtype embryos (n=3) to each genotype: Delta mutants (n=3), N+ mutants that had a higher level of Dl expression (n=3), and N^+ mutants with a very low level of Dl signal (n=3). Error bars represent standard deviation.

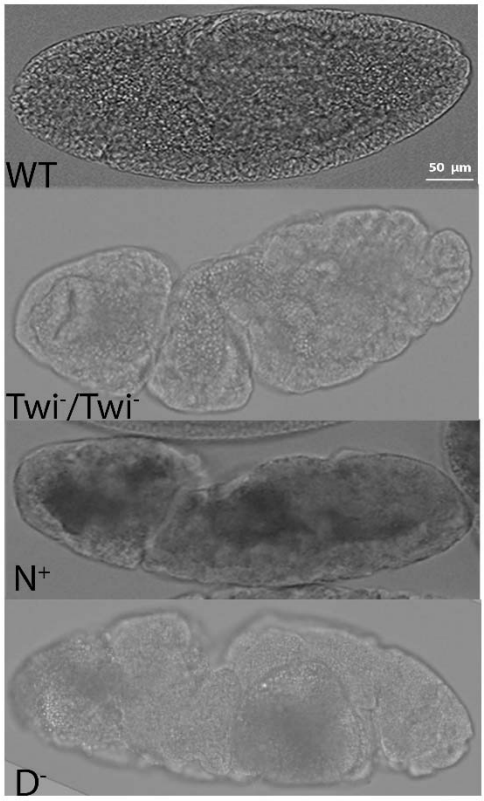

Supplementary figure 1. Bright field images of wildtype and mutant embryos at germband extension (stage 9-11). Loss-of-function Twist mutants have similar morphological defects as gain-of-function and loss of function mutants in the Notch signalling pathway such as aberrant invaginations along the AP axis and the overall twisted body phenotype.

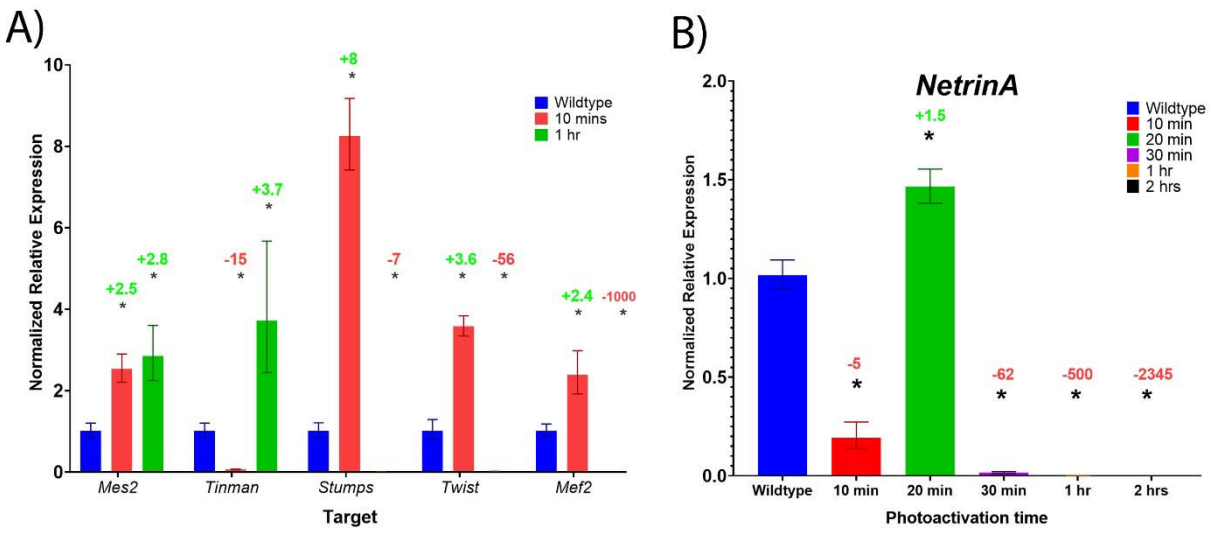

Supplementary figure 2. Expression of mesodermal genes in wildtype and Opto-NICD embryos following photoactivation for short durations. Normalized relative mRNA expression of mesodermal genes, n= 30 embryos at cephalic furrow formation in each genotype. Error bars represent SEM. Statistical significance is denoted by '*' (a p-value <0.05) determined from a two-tailed t-Test comparing wildtype embryos to Delta mutants and wildtypes to N+ mutants. A) shows expression in wildtype (blue bars), Opto-NICD embryos photoactivated for 10 minutes (red bars) and 1 hour (green bars). B) Shows *NetrinA* expression in wildtype (blue bar), Opto-NICD embryos photoactivated for 10 minutes (red bar), 20 minutes (green bar), 30 minutes (purple bar), 1 hour (orange bar), and 2 hours (black bar).